IEEE Photonics Journal
An IEEE Photonics Society Publication

Horizontal Directional Coupler Formed With Waveguides of Different Heights for Mode-Division Multiplexing

Volume 9, Number 5, October 2017

Wei Ke Zhao
Kai Xin Chen, *Member, IEEE*
Jie Yun Wu
Kin Seng Chiang, *Member, IEEE*

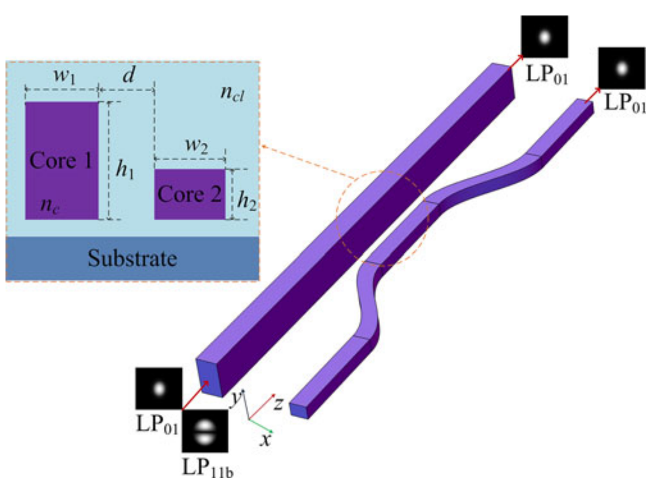

DOI: 10.1109/JPHOT.2017.2731046

Horizontal Directional Coupler Formed With Waveguides of Different Heights for Mode-Division Multiplexing

Wei Ke Zhao,[1] **Kai Xin Chen,**[1] ***Member, IEEE*****, Jie Yun Wu,**[1]
and Kin Seng Chiang,[1,2] ***Member, IEEE***

[1]Key Laboratory of Optical Fiber Sensing and Communications, University of Electronic Science and Technology of China, Chengdu 611731, China
[2]Department of Electronic Engineering, City University of Hong Kong, Hong Kong SAR, China

DOI:10.1109/JPHOT.2017.2731046

Manuscript received May 4, 2017; revised July 15, 2017; accepted July 19, 2017. Date of publication July 24, 2017; date of current version August 14, 2017. This work was supported in part by the National Natural Science Foundation of China under Grants U1533121, 61377057, and 61177054, in part by the State Key Laboratory of Integrated Optoelectronics at Jilin University, China under Projects IOSKL2014KF07 and IOSKL2016KF10, in part by the Open Fund of IPOC of BUPT under Project IPOC2016B007, and in part by the 111 Project of UESTC under Grant B14039. Corresponding author: Kai Xin Chen (e-mail: chenkx@uestc.edu.cn).

Abstract: We propose a horizontal directional coupler formed with two parallel waveguides of different heights. By breaking the symmetry in both the horizontal and the vertical direction, this directional coupler can be designed to allow us coupling between any two spatial modes of a few-mode waveguide, regardless of their symmetry properties, whereas a conventional directional coupler formed with planar waveguides of equal heights only allows us coupling between two spatial modes of the same symmetry in the vertical direction. As an example, we design and fabricate such a directional coupler with polymer material for the (de)multiplexing of the LP_{01} and the LP_{11b} mode, which have a symmetric and an antisymmetric field distribution in the vertical direction, respectively. Our typical fabricated device shows a coupling ratio higher than 95% in the wavelength range from 1530 to 1560 nm. The insertion losses for the LP_{01} and LP_{11b} modes are 9.6 and 12.8 dB, respectively. The performance of the device is weakly sensitive to temperature variations. The proposed directional coupler is easy to fabricate and can be used as a basic structure for the implementation of mode-controlling devices for mode-division-multiplexing applications.

Index Terms: Directional coupler, integrated optics, mode multiplexer, multiplexing, optical waveguide, polymer waveguide.

1. Introduction

Directional coupler (DC) formed with two parallel waveguides is a fundamental and essential structure in integrated optics [1]–[7]. With a DC, light can be transferred effectively between two waveguides and this phenomenon has been studied extensively over the years for the realization of a broad spectrum of devices, which include, for example, power distributors [1], [2], wavelength-division multiplexers [4], switches [5], polarization splitters [6], [7], and so on. In recent years, the structure of DCs has been applied to the implementation of mode (de)multiplexers for application in mode-division multiplexing (MDM) [8]–[17]. Limited by the fabrication processes for popular waveguide materials like glass and silicon, the two parallel waveguides of a conventional DC have the same height and the widths of the two waveguides are controlled to achieve the

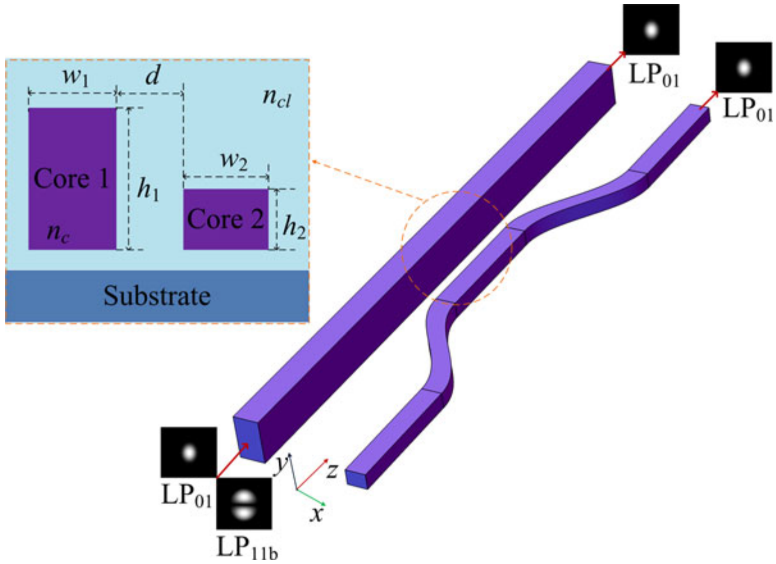

Fig. 1. Schematic diagram of the proposed DC-based LP_{01}-LP_{11b} mode (de)multiplexer with the inset showing the cross section of the coupling region.

phase-matching condition required for effective coupling between two different waveguide modes [8]–[15]. Such an asymmetric DC was first demonstrated for the (de)multiplexing of the LP_{01} and the LP_{11a} modes [8]. More spatial modes can be (de)multiplexed by cascading more DCs [9]–[11]. However, because the two waveguides have the same height, the DC cannot be used to (de)multiplex two spatial modes that have different symmetry properties in the vertical direction, e.g., the LP_{01} and the LP_{11b} modes, which have a symmetric and an anti-symmetric field distribution in the vertical direction, respectively. This problem can be solved by using a specially designed mode rotator to convert the LP_{11b} mode into the LP_{11a} mode, which has a symmetric field distribution in the vertical direction and can be coupled to the LP_{01} mode with the DC [10], [11]. The incorporation of mode rotators, however, adds significant complexity to the layout and the fabrication of the device. Another approach is the use of a vertical DC, where the two waveguides are placed in two different levels and, therefore, can have different heights and different widths [16]. A vertical DC can be designed to couple between two arbitrary spatial modes, but it requires a multi-layer structure and an accurate alignment of the waveguides in the vertical direction, which complicates the fabrication process. Nevertheless, a three-mode (de)multiplexer that combines a horizontal DC and a vertical DC [16] and a five-mode (de)multiplexer that integrates four cascaded vertical DCs were demonstrated recently [17]. Both devices were fabricated with polymer material.

In this paper, we propose a horizontal DC formed with two waveguides that have different heights. Such a DC can be designed to couple between any two spatial modes, regardless of their symmetry properties, and thus relax the constraint of the conventional horizontal DC. It is also much easier to fabricate this DC than a vertical DC. As a demonstration, we design and fabricate an LP_{01}-LP_{11b} mode (de)multiplexer with the proposed DC structure using polymer material. Our typical fabricated device shows a coupling ratio higher than 95% in the wavelength range from 1530 nm to 1560 nm (with a maximum value of 99.1% at the wavelength 1540 nm). We also characterize the polarization and the temperature dependence of the performance of the device. Our proposed DC can be used as a basic unit for the implementation of various mode-controlling devices for MDM applications.

2. Principle and Design

The proposed horizontal DC with unequal waveguides heights is shown schematically in Fig. 1. The DC consists of a two-mode waveguide core (TMW) with width w_1 and height h_1, which supports the

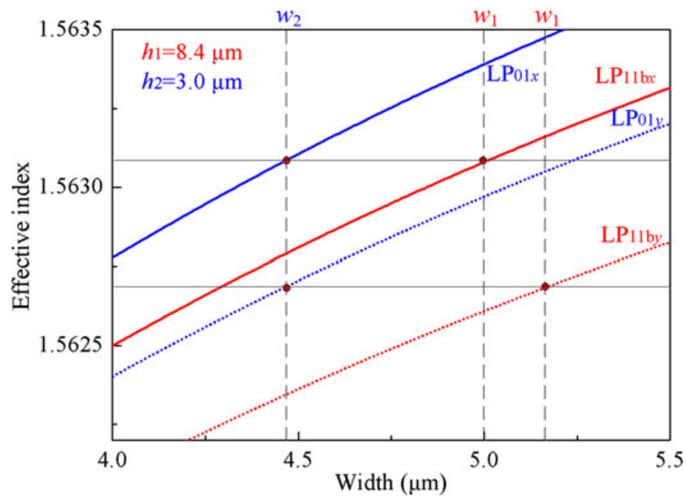

Fig. 2. Variations of the effective indices of the LP_{01} mode of the SMW and the LP_{11b} mode of the TMW with the core widths, calculated at 1550 nm for the x- and the y-polarization.

LP_{01} and the LP_{11b} mode, and a single-mode waveguide core (SMW) with width w_2 and height h_2, which supports only the LP_{01} mode. In the coupling region, the two cores are parallel and separated by a distance *d*. The two cores are gradually branched out towards the two ends with S-bends. The refractive indices of the cores and the surrounding cladding are denoted as n_c and n_{cl}, respectively.

For the DC to operate as an ideal mode (de)multiplexer, the LP_{11b} mode launched into the TMW should be coupled completely to the LP_{01} mode of the SMW, while the LP_{01} mode launched in the TMW should stay in the TMW. To achieve maximum coupling between the LP_{11b} mode of the TMW and the LP_{01} mode of the SMW, the effective indices of the two modes must be equal, i.e., the two modes must be phase-matched, and the length of the coupling region must be optimized. In our design, the refractive index of the cladding is 1.5595 for both polarizations, while that of the cores is 1.5716 for the *x*-polarization (quasi-TE polarization) or 1.5709 for the *y*-polarization (quasi-TM polarization). These are the measured refractive indices for the polymer materials used in our experiments. We fix the heights of the two cores at $h_1 = 8.4\,\mu$m and $h_2 = 3.0\,\mu$m and vary the widths of the two cores to search for the phase-matching condition. We calculate the effective indices and the field distributions of the modes with the commercial mode solver COMSOL.

Fig. 2 shows the variations of the effective indices of the modes of the two waveguides with the core widths at the wavelength 1550 nm, where the curves labelled as "LP_{01x}" and "LP_{01y}" are the dispersion curves for the *x*-polarized and *y*-polarized LP_{01} modes of the SMW, respectively, and those labelled as "LP_{11bx}" and "LP_{11by}" are the dispersion curves for the *x*-polarized and *y*-polarized LP_{11b} modes of the TMW, respectively. As shown in Fig. 2, for the *x*-polarization, the LP_{01} mode of the SMW and the LP_{11b} mode of the TMW have equal effective index 1.5631 (i.e., they are phase-matched), when $w_1 = 5.0\,\mu$m and $w_2 = 4.4\,\mu$m. For the *y*-polarization, the two modes are phase-matched, when $w_1 = 5.2\,\mu$m and $w_2 = 4.4\,\mu$m. Our DC is designed to optimize the performance for the *x* polarization. The large polarization dependence in the phase-matching condition is caused by the large birefringence in the core material; it is not a characteristic of the DC structure. Polarization-insensitive operation can be obtained if the material birefringence is small.

The performance of the DC is governed by two mode coupling ratios: the coupling ratio between the LP_{11b} mode of the TMW and the LP_{01} mode of the SMW, denoted as Cr_{11b}, and the coupling ratio between the LP_{01} mode of the TMW and the LP_{01} mode of the SMW, denoted as Cr_{01}, which are given by

$$Cr_{11b} = \frac{P_S(11b)}{P_T(11b) + P_S(11b)} \tag{1}$$

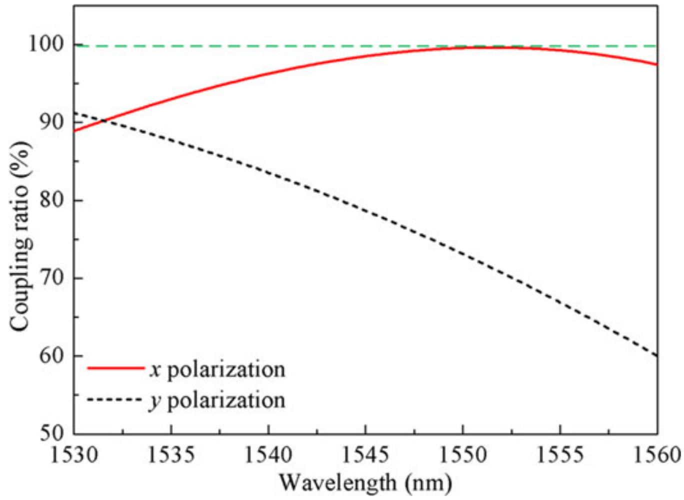

Fig. 3. Wavelength dependences of the coupling ratios Cr_{11b}.

$$Cr_{01} = \frac{P_S(01)}{P_T(01) + P_S(01)} \tag{2}$$

where $P_T(11b)$ and $P_S(11b)$ are the output powers from the TMW and the SMW, respectively, when only the LP_{11b} mode is launched into the TWM; and $P_T(01)$ and $P_S(01)$ are the output powers from the TMW and the SMW, respectively, when only the LP_{01} mode is launched into the TWM. For the DC to function as a mode (de)multiplexer, the value of Cr_{11b} should be as large as possible and that of Cr_{01} should be as small as possible. Any of the LP_{11b} mode power launched into the TMW that is not coupled to the SMW, i.e., $Cr_{11b} < 1$, represents crosstalk to the LP_{01} mode channel, while any of the LP_{01} mode power launched into the TMW that is coupled to the SMW, i.e., $Cr_{01} > 0$, represents crosstalk to the LP_{11b} mode channel. In practice, the crosstalk from the LP_{11b} mode to the LP_{01} mode can be completely eliminated by introducing a taper along the TMW at the demultiplexing end of the DC. With such a taper, $Cr_{11b} < 1$ just gives rise to an additional loss for the LP_{11b} mode. The crosstalk from the LP_{01} mode to the LP_{11b} mode is simply given by Cr_{01}/Cr_{11b}.

In our study, we employ a 3D finite-difference beam propagation method (3DFD-BPM) (BeamPROP, RSoft) to search for the length of the coupling region required for maximizing the value of Cr_{11b} (which is referred to as the coupling length of the DC) at a given core separation d. In the simulation, the output powers of specific modes (the LP_{01} and LP_{11b} modes) required for the calculation of the coupling ratios are obtained by projecting the output field on the respective modes. In our design, we choose $d = 4.5\,\mu$m. Each S-bend has a longitudinal length of 4500 μm, which provides a final core separation of 127 μm. Given the S-bend parameters, the optimal length of the straight section of the SMW for maximizing the value of Cr_{11b} for the *x* polarization is 3900 μm at the wavelength 1550 nm. The parameters of the S-bends are not critical, as we can always adjust the length of the straight section to maximize the coupling ratio. Fig. 3 shows the wavelength dependence of the Cr_{11b} value over the wavelength range 1530–1560 nm. For the *x*-polarization, the coupling ratio Cr_{11b} is 100% at 1550 nm and drops to 89% at 1530 nm and 96% at 1560 nm, while, for the *y*-polarization, the coupling ratio Cr_{11b} is 91% at 1530 nm and decreases monotonically to 60% at 1560 nm. The large difference between the effective indices of the LP_{01} modes of the SMW and the TMW results in a very small Cr_{01} (< -55 dB), and, therefore, the crosstalk from the LP_{01} mode to the LP_{11b} mode is negligible for both polarizations.

Fig. 4(a) and (b) show the propagations of the LP_{01} mode and the LP_{11b} mode along the DC, respectively, where both modes are launched into the TMW. The results are calculated for the *x*-polarization at the wavelength 1550 nm, assuming two parallel straight waveguides. As shown in Fig. 4(a), the LP_{01} mode stays in the TMW along the device, while the LP_{11b} mode is completely coupled to the LP_{01} mode of the SMW.

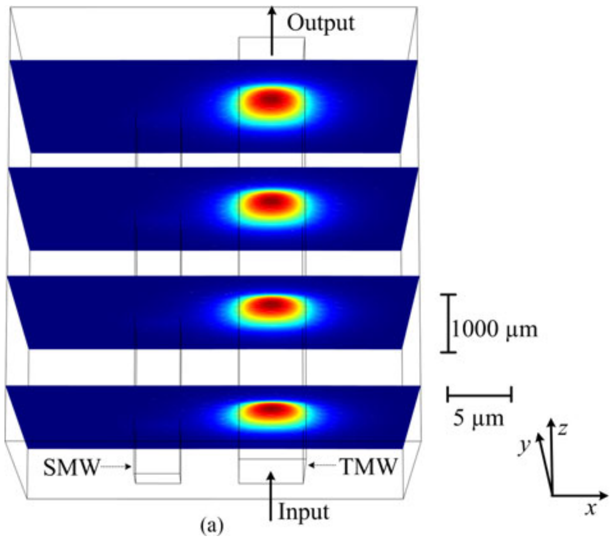

Fig. 4. Propagation of (a) the LP_{01} mode and (b) the LP_{11b} mode along the DC, where they are launched into the TMW, respectively.

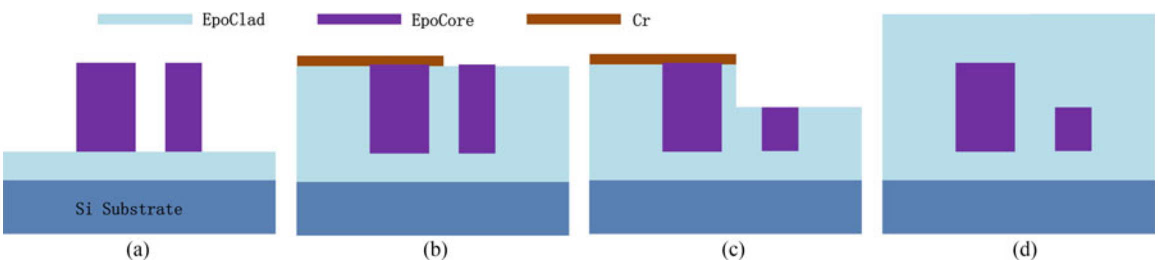

Fig. 5. Major steps in the fabrication the proposed DC: (a) forming two cores with the same height; (b) covering the TMW core with a Cr mask; (c) etching the height of the SMW core; and (d) completing the process by coating both cores.

3. Fabrication and Measurement

We followed the design parameters as closely as possible in the fabrication of the DC. The polymer materials used were EpoClad and EpoCore (Micro Resist Technology), which were used as the cladding and the core material, respectively. The refractive indices of these materials in thin-film form were measured at the wavelength 1538 nm with a commercial prism coupler system (Metricon 2010). The refractive indices of the EpoClad film were 1.5595 for both polarizations, and the refractive index of the EpoCore film was 1.5716 for the *x*-polarization and 1.5709 for the *y*-polarization. These materials have been used previously for making 3D waveguide structures [16], [17] and proven to be highly stable and durable, though they are developed mainly for application at 850 nm [18].

The proposed DC was fabricated by the standard photolithography technique and oxygen reactive ion etching (RIE) as shown in Fig. 5(a)–(d). An EpoClad film was first spin-coated and cured onto an oxidized Si substrate to a thickness of $\sim$12 μm as the lower cladding. An EpoCore film was next spin-coated onto the lower cladding to a thickness of 8.4 μm. With the standard photolithography process, the EpoCore film was chemically etched into the pattern of the device, as shown in Fig. 5(a). An EpoClad cladding was then spin-coated onto the cores and a Cr film as a mask was formed on the TMW core by sputtering and chemical etching, as shown in Fig. 5(b). The SMW core was then etched to a thickness of 3.0 μm with RIE, as shown in Fig. 5(c). After the residual Cr mask was removed, a $\sim$12 μm thick Epoclad was finally spin-coated onto the device and cured, as shown

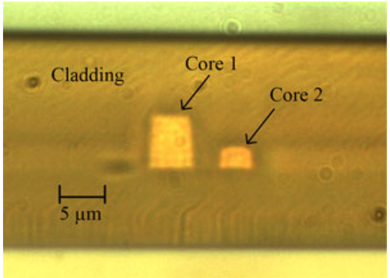

Fig. 6. Microscopic image showing the cross section of the coupling region of a typical fabricated DC.

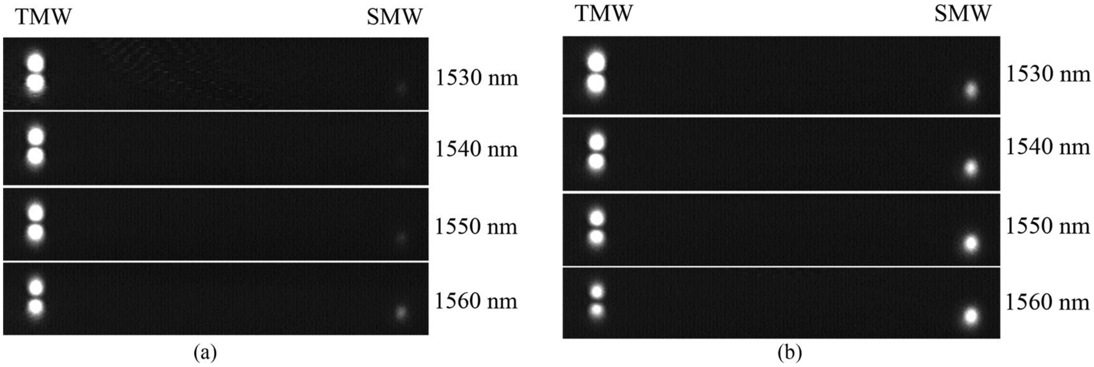

Fig. 7. Output near-field images taken for (a) the *x*-polarization and (b) the *y*-polarization at different wavelengths, when the LP_{01} mode was launched into the SMW.

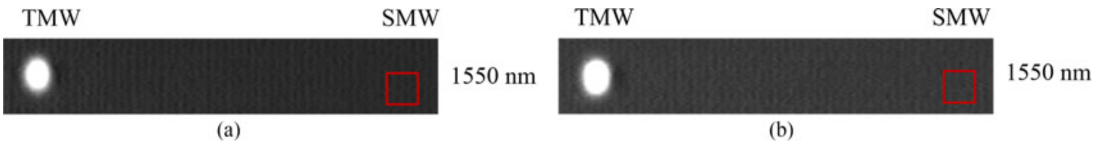

Fig. 8. Output near-field images taken for (a) the *x*-polarization and (b) the *y*-polarization at 1550 nm, when the LP_{01} mode was launched into the TMW.

in Fig. 5(d). We fabricated a number of identical devices, each of which had a length of ~1.3 cm. Fig. 6 is the microscopic image of the cross section of the coupling region of a typical fabricated DC. The slight deviations from perfect rectangular cores caused by the fabrication process should not significantly affect the performance of the DC.

To inspect the mode coupling characteristics of the fabricated DC, the light from a tunable laser (Santur TL-2020-C-107) was made to pass through a polarization controller (PC) first and then launched into the SMW with a lensed single-mode fiber (SMF) to excite the LP_{01} mode. The output near-field images were captured with an infrared camera (MicronViewer, Model 7290A) over the wavelength range 1530–1560 nm and shown in Fig. 7(a) and (b) for the *x*- and the *y*-polarization, respectively. For the *x*-polarization, the LP_{01} mode of the SMW is almost completely coupled to the LP_{11b} mode of the TMW at the wavelength 1540 nm, as shown in Fig. 7(a), while, for the *y*-polarization, only a portion of the LP_{01} mode is coupled to the LP_{11b} mode of the TMW, as shown in Fig. 7(b). These results agree with our expectation that the DC should perform better for the *x*-polarization.

Fig. 8(a) and (b) show the output near-field images taken at 1550 nm for the *x*- and the *y*-polarization, respectively, when the LP_{01} mode was launched into the TMW by carefully aligning a two-mode fiber to the TMW. As expected, little light is coupled to the SMW.

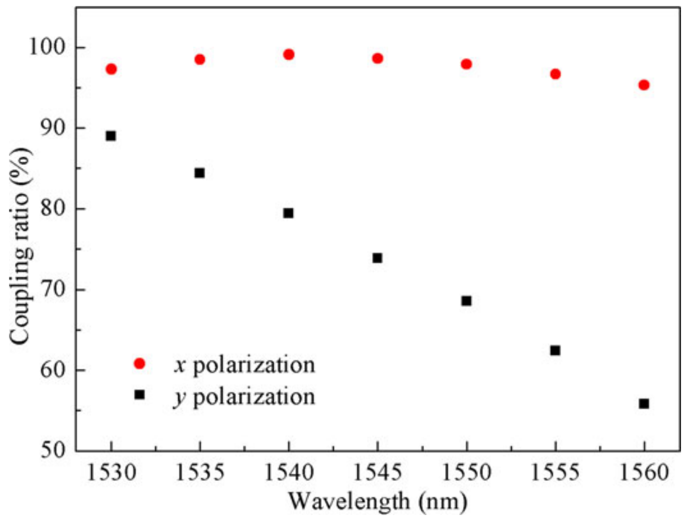

Fig. 9. Coupling ratio Cr_{11b} measured for a typical fabricated device at 24 °C.

The coupling ratios Cr_{11b} of Cr_{01} of the fabricated device can be deduced from the output powers measured from the TMW and the SMW, when the LP_{01} or the LP_{11b} mode was selectively launched into the TMW. To launch the LP_{11b} mode into the TMW, an all-fiber LP_{01}–LP_{11} mode converter was used [19]. The coupling ratio Cr_{11b} over the wavelength range 1530–1560 nm, measured at 24 °C, is shown in Fig. 9. For the *x*-polarization, the coupling ratio Cr_{11b} is higher than 95% over the range 1530–1560 nm and has a maximum value of 99.1% at 1540 nm, while, for the *y*-polarization, it has a maximum value of 89% at 1530 nm and decreases monotonically to ∼55% at 1560 nm. On the other hand, the coupling ratio Cr_{01} was measured to be lower than 0.5% over the range 1530–1560 nm for both polarizations. A comparison of Figs. 3 and 9 shows that the experimental results agree well with the theoretical results.

By applying the cut-back method to straight reference waveguides that had the same parameters as the SMW and the TMW, the propagation losses of the LP_{01} mode of the SMW, the LP_{01} mode of the TMW, and the LP_{11b} mode of the TMW were measured to be 5.1 dB/cm, 2.5 dB/cm, and 3.3 dB/cm, respectively, at the wavelength1550 nm. The larger loss of the SMW is attributed to its smaller core size and the increased surface roughness by the RIE process. The insertion losses of the LP_{01} and the LP_{11b} mode of the TMW, with one end of the device connected to a two-mode fiber and the other end connected to a SMF, were measured to be 9.6 dB and 12.8 dB, respectively.

The temperature sensitivity of the device for the *x*-polarization was also measured by controlling the operation temperature of the device with a hot plate placed under the device. Fig. 10 shows the wavelength dependences of the coupling ratio Cr_{11b} measured at different temperatures. The effects of temperature variations on the performance of the device are complicated. A change in the temperature can change the effective indices of the modes and the interaction length of the device and eventually the coupling ratio. These effects may reinforce or counteract each other in terms of changing the coupling ratio at a specific wavelength (depending on whether the interaction length is longer or shorter than the ideal coupling length). While a temperature change can in general cause a shift in the wavelength at which maximum mode coupling occurs, the trend is not linear. It can be seen that almost 100% coupling can be achieved at the wavelength 1560 nm at 22.5 °C. Over the temperature range 15–60 °C, the maximum (minimum) value of Cr_{11b} at each temperature is not lower than 92% (82%) in the wavelength range 1530–1560 nm. Regardless of the fact that the polymer material has a large thermo-optic coefficient and thermal expansion coefficient, compared with other common waveguide material systems, the performance of our polymer DC is not particularly sensitive to temperature variations.

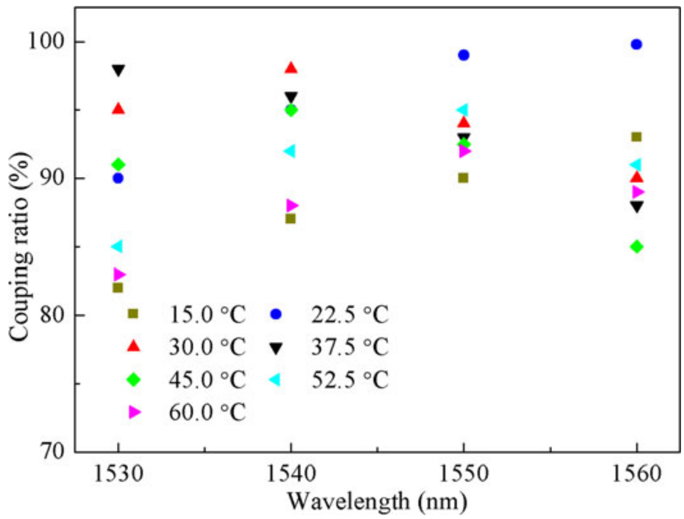

Fig. 10. Coupling ratio Cr_{11b} measured at different temperatures for the *x*-polarization.

4. Conclusion

We have proposed and demonstrated a horizontal DC structure where the two parallel waveguide cores have different heights. This DC allows coupling between two modes with arbitrary symmetry properties and thus removes a serious constraint of the conventional DC where the two parallel waveguide cores have the same height. As an example, we have designed and fabricated such a DC for coupling between the LP_{01} and the LP_{11b} mode with polymer materials. Our typical fabricated DC has a length of ~1.3 cm and shows a coupling ratio higher than 95% in the wavelength range 1530–1560 nm. The insertion losses of the DC with fibers connected at both ends are 9.6 dB and 12.8 dB for the LP_{01} and the LP_{11b} mode, respectively, which are mainly due to the material loss [16], [17]. It should be possible to significantly reduce the insertion losses by using low-loss polymer material developed for the C-band. The performance of the DC is only weakly sensitive to the ambient temperature. Our proposed DC can be used as a building block for the implementation of mode-controlling devices for MDM applications. While we have demonstrated the proposed DC with polymer material for its advantages of easy fabrication and low cost [18], [20], the same structure can also be implemented with other material platforms, such as InP, SiN, and Si, for the realization of more advanced integrated photonic circuits.

References

[1] E. A. J. Marcatili, “Dielectric rectangular waveguide and directional coupler for integrated optics,” *Bell Labs Techn. J.*, vol. 48, no. 7, pp. 2071–2102, Mar. 1969.
[2] H. Kogelnik and R. Schmidt, “Switched directional couplers with alternating ΔB,” *IEEE J. Quantum Electron.*, vol. QE-12, no. 7, pp. 396–401, Jul. 1976.
[3] K. S. Chiang, “Theory of pulse propagation in optical directional couplers,” *J. Nonlin. Opt. Phys. Mater.*, vol. 14, no. 2, pp. 133–147, Nov. 2004.
[4] K. Kitayama and Y. Ishida, “Wavelength-selective coupling of two-core optical fiber: Application and design,” *J. Opt. Soc. Amer. A*, vol. 2, no. 1, pp. 90–94, Jan. 1985.
[5] K. X. Chen, P. L. Chu, K. S. Chiang, and H. P. Chan, “Design and fabrication of a broadband polymer vertically-coupled optical switch,” *J. Lightw. Technol.*, vol. 24, no. 2, pp. 904–911, Feb. 2006.
[6] K. X. Chen, P. L. Chu, K. S. Chiang, and H. P. Chan, “Design and fabrication of a three dimensional polymer optical waveguide polarization splitter,” *Opt. Commun.*, vol. 250, pp. 297–301, Feb. 2005.
[7] D. X. Dai, “Silicon polarization beam splitter based on an asymmetrical evanescent coupling system with three optical waveguides,” *J. Lightw. Technol.*, vol. 30, no. 20, pp. 3281–3287, Oct. 2012.
[8] N. Hanzawa, K. Saitoh, T. Sakamoto, T. Matsui, S. Tomita, and M. Koshiba, “Asymmetric parallel waveguide with mode conversion for mode and wavelength division multiplexing transmission,” in *Proc. Int. Conf. Opt. Fiber Commun /Nat. Fiber Opt. Eng.*, Los Angeles, CA, USA, 2012, Paper OTu1I.4.

[9] D. X. Dai, J. Wang, and Y. C. Shi, “Silicon mode (de)multiplexer enabling high capacity photonic networks-on-chip with a single-wavelength-carrier light,” *Opt. Lett.*, vol. 38, no. 9, pp. 1422–1424, May 2013.
[10] K. Saitoh *et al.*, “PLC-based LP_{11} mode rotator for mode-division multiplexing transmission,” *Opt. Exp.*, vol. 22, no. 16, pp. 19117–19130, Aug. 2014.
[11] N. Hanzawa *et al.*, “Demonstration of PLC-based six-mode multiplexer for mode division multiplexing transmission,” in *Proc. Euro. Conf. Opt. Commun.*, Valencia, Spain, 2015, Paper no. P2.5.
[12] Y. H. Ding, J. Xu, F. D. Ros, B. Huang, H. Y. Ou, and C. Peucheret, “On-chip two-mode division multiplexing using tapered directional coupler-based mode multiplexer and demultiplexer,” *Opt. Exp.*, vol. 21, no. 8, pp. 10376–10382, Apr. 2013.
[13] J. W. Liao *et al.*, “Mode splitter without changing the mode order in SOI waveguide,” *IEEE Photon. Technol. Lett.*, vol. 28, no. 22, pp. 2597–2600, Nov. 2016.
[14] Y. Sun, Y. Xiong, and W. N. Ye, “Experimental demonstration of a two-mode (de)multiplexer based on a taper-etched directional coupler,” *Opt. Lett.*, vol. 41, no. 16, pp. 3743–3746, Aug. 2016.
[15] H. Y Qiu *et al.*, “Silicon add-drop filter based on multimode grating assisted couplers,” *IEEE Photon. J.*, vol. 8, no. 6, Dec. 2016, Art. no. 7805308.
[16] J. Dong, K. S. Chiang, and W. Jin, “Compact three-dimensional polymer waveguide mode multiplexer,” *J. Lightw. Technol.*, vol. 33, no. 22, pp. 4580–4588, Sep. 2015.
[17] Q. Huang, Y. Wu, W. Jin, and K. S. Chiang, “Five-mode multiplexer based on cascaded vertical directional couplers,” in *Proc. 2016 Int. Conf. IEEE Photon.*, Waikoloa, HI, USA, Oct. 2–6, 2016, Paper MD4.1.
[18] W. Jin, K. S. Chiang, K. P. Lor, H. P. Chan, J. T. L. To, and R. H. M. Leung, “Industry compatible embossing process for the fabrication of waveguide embedded optical printed circuit boards,” *J. Lightw. Technol.*, vol. 31, no. 24, pp. 4045–4050, Dec. 2013
[19] J. Dong and K. S. Chiang, “Temperature-insensitive mode converters with CO_2 -Laser written long-period fiber gratings,” *IEEE Photon. Technol. Lett.*, vol. 27, no. 9, pp. 1006–1009, May 2015.
[20] J. Chen *et al.*, “High-bandwidth and large coupling tolerance graded-index multimode polymer waveguides for on-board high-speed optical interconnects,” *J. Lightw. Technol.*, vol. 34, no. 12, pp. 2934–2940, Nov. 2015.